

Experimental Measurements and Molecular Simulation of Carbon Dioxide Adsorption on Carbon Surface

Ibrahim Gomaa, Javier Guerrero, Zoya Heidari, and D. Nicolas Espinoza, The University of Texas at Austin

Copyright 2022, Society of Petroleum Engineers DOI 10.2118/210264-MS

This paper was prepared for presentation at the 2022 SPE Annual Technical Conference and Exhibition held in Houston, Texas, USA, 3 - 5 October 2022.

This paper was selected for presentation by an SPE program committee following review of information contained in an abstract submitted by the author(s). Contents of the paper have not been reviewed by the Society of Petroleum Engineers and are subject to correction by the author(s). The material does not necessarily reflect any position of the Society of Petroleum Engineers, its officers, or members. Electronic reproduction, distribution, or storage of any part of this paper without the written consent of the Society of Petroleum Engineers is prohibited. Permission to reproduce in print is restricted to an abstract of not more than 300 words; illustrations may not be copied. The abstract must contain conspicuous acknowledgment of SPE copyright.

Abstract

Geological storage of carbon dioxide (CO₂) in depleted gas reservoirs represents a cost-effective solution to mitigate global carbon emissions. The surface chemistry of the reservoir rock, pressure, temperature, and moisture content are critical factors that determine the CO₂ adsorption capacity and storage mechanisms. Shale-gas reservoirs are good candidates for this application. However, the interactions of CO₂ and organic content still need further investigation. The objectives of this paper are to (i) experimentally investigate the effect of pressure and temperature on the CO₂ adsorption capacity of activated carbon, (ii) quantify the nanoscale interfacial interactions between CO₂ and the activated carbon surface using Monte Carlo molecular modeling, and (iii) quantify the correlation between the adsorption isotherms of activated carbon-CO₂ system and the actual carbon dioxide adsorption on shale-gas rock at different temperatures and geochemical conditions. Activated carbon is used as a proxy for kerogen. The objectives aim at obtaining a better understanding of the behavior of CO₂ injection and storage into shale-gas formations.

We performed experimental measurements and Grand Canonical Monte Carlo (GCMC) simulations of CO₂ adsorption onto activated carbon. The experimental work involved measurements of the high-pressure adsorption capacity of activated carbon using pure CO₂ gas. Subsequently, we performed a series of GCMC simulations to calculate CO₂ adsorption capacity on activated carbon to validate the experimental results. The simulated activated carbon structure consists of graphite sheets with a distance between the sheets equal to the average actual pore size of the activated carbon sample. Adsorption isotherms were calculated and modeled for each temperature value at various pressures.

The adsorption of CO₂ on activated carbon is favorable from the energy and kinetic point of view. This is due to the presence of a wide micro to meso pore sizes that can accommodate a large amount of CO₂ particles. The results of the experimental work show that excess adsorption results for gas mixtures lie in between the results for pure components. The simulation results agree with the experimental measurements. The strength of CO₂ adsorption depends on both surface chemistry and pore size of activated carbon. Once strong adsorption sites within nanoscale network are established, gas adsorption even at very low pressure is governed by pore width rather than chemical composition. The outcomes of this paper provides new insights about the parameters affecting CO₂ adsorption and storage in shale-gas reservoirs, which is critical for developing standalone representative models for CO₂ adsorption on pure organic carbon.

Introduction

Global warming is considered the greatest environmental challenge facing the planet Earth recently. According to the National Oceanic and Atmospheric Administration (NOAA), the global average temperature should be maintained at 1.5 °C above the preindustrial average in order to stabilize the Earth's climate, terrestrial and aquatic system (Steffen et al. 2018; He et al. 2022). The current levels of atmospheric CO₂ are responsible for approximately 26% of global warming (Bhui 2021). Hence, reducing the concentrations of CO₂ has become a substantial need to reduce the greenhouse gas effects and prevent the continuous increase in Earth's surface temperature. Considerable reduction in CO₂ emissions coming from the global energy system is only feasible over the long term investments in the clean energy sectors (Johansson et al. 1996). In the meantime, the world energy consumption is predicted to double in the coming ten years (Lau et al. 2021). This in turn would increase the demand on fossil fuel resources that are considered a main source of CO₂ emissions. Carbon capture and sequestration (CCS) holds a great promise for immediately deceasing the atmospheric CO₂ concentrations and limit the greenhouse gas emissions under the current energy regime (Edmonds et al. 2002). This process starts by collecting CO₂ from intensive point sources, such as power plants and industrial facilities and then transported and stored in deep underground reservoirs. Depleted shale-gas reservoirs (Li et al. 2006; Shirbazo et al. 2021), deep saline formations (Kumar et al. 2005; Vilarrasa et al. 2010), and coalbeds (White et al. 2003; Shi and Durucan 2005) are typical geological structures for CO₂ sequestration.

Shale-gas reservoirs have been considered as attractive CO₂ sequestration options due to their widespread and high capacity of CO₂ adsorption on the surface of solid rock constituents (Shirbazo et al. 2021). Khosrokhavar et al. (2014) showed that shale-gas formations have a more significant potential in storing CO₂ gas than saline formations and coalbeds due to the dangers of induced seismicity associated with CO₂ injection into these latter structures. The authors claimed that depleted shale-gas reservoirs have the suitable infrastructure of injection wells and transportation pipelines that make the process of CO₂ injection more viable. Tayari et al. (2015) and Boosari et al. (2015) provided both technical and economic studies about the viability of CO₂ storage in unconventional shale-gas reservoirs. Their results showed that despite of the extreme low permeability of such formations, shale-gas reservoirs typically contain natural and hydraulic fractures, which allow them to store large amounts of CO₂. Merey and Sinayuc (2016) carried out gas adsorption experiments on both BPL activated carbon and Dadas shale samples at temperatures ranging from 25 °C to 75 °C and pressures up to 2000 psia using both pure CO₂ and methane (CH₄) gases. They used both Langmuir isotherm and Ono-Kondo lattice models to evaluate the experimental results and construct the adsorption isotherms for shale-gas reservoirs. They emphasized on the inverse relationship between temperature and gas adsorption capacity for shale reservoirs. Moreover, they pointed out that shale-gas reservoirs are good candidates for storing CO₂ in the forms of free and adsorbed gas. Liu et al. (2020) presented a numerical model based on embedded discrete fracture model (EDFM) to investigate the capacity of CO₂ sequestration in shale-gas reservoirs in the macroscopic scale. The results showed that the location, distribution, and connectivity of the fractures have critical effects on the adsorption capacity of the shale reservoirs.

Shales are fine-grained sedimentary formations that contain organic matter, inorganic matter, and natural/hydraulic fractures. This multiscale pore system offers different gas transport and storage mechanisms (Yao et al. 2013; Wang et al. 2021). According to the IUPAC, shale porosity is classified as mi croporosity (pore size <2 nm), mesoporosity (pore size 2–50 nm), and macroporosity (pore size >50 nm) (Kuila and Prasad 2013). The higher the content of both micro and meso pores, the higher the gas adsorption capacity within the pore structure (Chalmers and Bustin 2008). Reservoir temperature has an inverse impact on the CO₂ adsorption as adsorption capacity decreases with a rise in temperature. This is attributed to the exothermic nature of the adsorption process (Zhou et al. 2019). Depending on the total organic carbon content (TOC),

maturity level, type of kerogen, as well as the clay content, gas adsorption capacity of shale formations can reach up to 85%. In order to understand how the mineral constituents of shale-gas formations affect CO₂ adsorption, Heller and Zoback (2014) performed CO₂ adsorption experiments on pure carbon, illite, and kaolinite samples. They emphasized on the analogous relationship between the overall adsorption behavior of CO₂ on Montery, Marcellus, and Eagle Ford shale samples and their relative constituting carbon and clay content. Hence, evaluating the adsorption isotherms of CO₂ gas on pure minerals such as carbon and clay minerals would lead to a better understanding of the behavior of CO₂ injection in shale-gas reservoirs.

Physical adsorption is the dominant adsorption mechanism by which CO₂ particles are attracted to the mineral/organic-matter solid interface in shale-gas reservoirs. These adsorbed molecules form a highdensity distinct gas phase that differ from the surrounding free gas (Zhang et al. 2018). Adsorption isotherms in shale formations, which describes the amount of gas adsorbed at different values of pressures at constant temperature, depend highly on the percentage and structure of the carbon content. However, the kerogen components and microstructure are quite complex to simulate (Wang et al. 2021). In addition, the heterogeneity and complex pore structure do not allow fully understanding of the adsorption mechanisms attributed to the solid-fluid interface of the mineral/organic-matter constituents of shale formations. Therefore, many studies used simple graphite sheets (Mosher et al. 2013; Zhang et al. 2017a, b; Cristancho-Albarracin et al. 2017) and activated carbon structures (Liu and Wilcox 2012; Zhan et al. 2015; Sandoval et al. 2018) to simulate the adsorption process of gases and liquids on the surface of shale rock. However, such studies did not integrate the experimental and molecular simulation approaches in their analysis. Such combination can potentially evaluate the validity of the modeling results and allow using generated models to simulate extreme reservoir conditions with confidence. Moreover, the power of the computation tools coming with molecular simulation models permits the ability to visually and statistically explain the adsorption isotherms in the molecular-scale domain.

Grand canonical Monte Carlo (GCMC) simulations are the most widely used approaches to study the adsorption properties of pure gases and their mixtures on porous materials (Yun et al. 2002). In the grand canonical ensemble, the system temperature, volume and chemical potential was kept constant (μ , V, T = Constant), while the number of molecules in the adsorbed phase is allowed to fluctuate. This mimics the adsorption experiments where the temperature and chemical potential of the gas species inside and outside the adsorbent material are equal and under equilibrium (Zhang et al. 2018). Aljamaan et al. (2017) used GCMC simulations to model the adsorption of gas mixtures on the surface of parallel planar graphitic surfaces. Jagadisan et al. (2021) constructed the adsorption isotherm of CH₄ on kerogen matrix using the GCMC at 300 K with pressure range of 1 MPa to 20 MPa.

In this paper, we experimentally evaluate the CO₂ adsorption isotherm on activated carbon under single temperature of 300 K and pressure range of 0.5 MPa to 6 MPa. Next, we build a molecular structure to physically and chemically represent activated carbon structure. GCMC simulations are then used to simulate and cross-validate the experimental results of CO₂ adsorption on activated carbon structures under the same pressure and temperature conditions. This validation enables the option of going beyond the experimental pressure and temperature limitations by performing dependable modeling. Finally, we explore the impacts of various geochemical and environmental conditions on adsorption behavior of CO₂ on activated carbon adsorption.

Materials and Methods

We carried out CO₂ adsorption experiments on activated carbon samples at 300 K. The samples were then characterized to get its surface area and average pore size. We then developed and validated a molecular model to mimic the actual carbon samples. Next, we matched the experimental CO₂ adsorption isotherm using GCMC simulations at the same temperature point (300 K). Finally, we performed sensitivity analyses

on the impact of temperature and chemical composition of the activated carbon model on the adsorption isotherms under different reservoir conditions.

Experimental Work

The experimental work starts with characterizing the physical properties of activated carbon sample including density, surface area and particle size. Then we show the used high-pressure adsorption setup and explain the theoretical part beyond the setup calibration and actual measurements.

Adsorbent sample characterization. We used medical grade activated carbon made from coconut shells provided by Envirosupply & Service. The coal particles have a total surface area $1150 - 1250 \text{ m}^2/\text{g}$, maximum ash content of 3% and apparent density $0.50 - 0.52 \text{ g/cm}^3$ (provided by manufacturer). The granular material passes sieve #5 (4mm) and is retained by sieve #10 (2mm).

High-pressure adsorption manometric setup. We designed a manometric apparatus to measure adsorption at high pressure. The setup consists of a sample cell (SC) and reference cell (RC) connected to an electromechanical syringe pump and source gases. The volume of the reference cell is 33.719 cm³. The sample cell has a capacity of 18.281 cm³ and it can store granular samples as well as core samples with maximum dimensions of 5 cm (2 in) in length and 2.54 cm (1 in) diameter. We used a Teledyne Isco Dseries 500x syringe pump with a cylinder capacity of 500 cm³. A pressure transducer (Rosemount 2088) monitors the pressure continuously. Fig. 1 presents a schematic of the manometric setup. Similar designs of manometric setups are available elsewhere (Hemert et al. 2009).

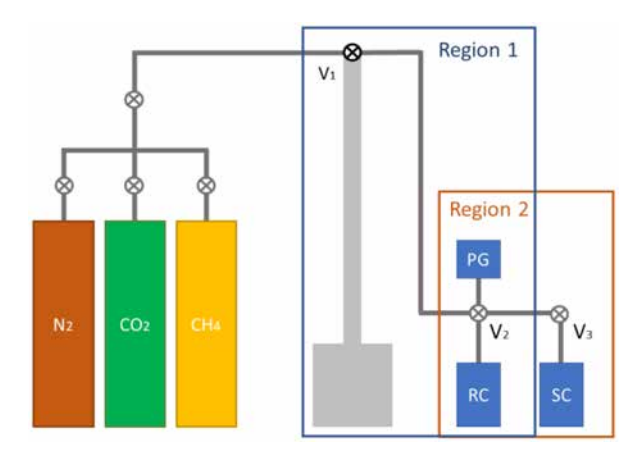


Figure 1—Schematic of the high-pressure adsorption setup. Components: reference cell (RC), sample cell (SC), valves (V_1, V_2, V_3) , pressure transducer (PG). V_1 is connected to an electromechanical syringe pump and the source gases.

Setup calibration. We first calibrated the high-pressure manometric setup for measuring pore volume in the absence of adsorption. The determination of solid volume by gas expansion follows Boyle's law. We calibrated the setup using five aluminum disks of known volume and research grade helium. Additional information about this method can be found elsewhere (Hemert et al. 2009).

According to Boyle's law, the product between pressure and volume at constant temperature is constant. Therefore, equating initial and final conditions can be expressed as

$$P_f(V_1 + V_2 - V_{sm}) = P_1 V_1 + P_2(V_2 - V_{sm}). \tag{1}$$

We can re-write Eq. 1 to obtain an expression for the volume of solids V_{sm} via

$$V_{sm} = \frac{P_f V_1 + P_f V_2 - P_1 V_1 - P_2 V_2}{P_f - P_2}. (2)$$

Measurement of adsorption amount. We measured high-pressure adsorption capacity of nanoporous activated carbon using CO_2 gas. Fig. 2 shows the manometric setup, including the reference cell, sample cell and solid sample with skeletal volume V_{sk} .

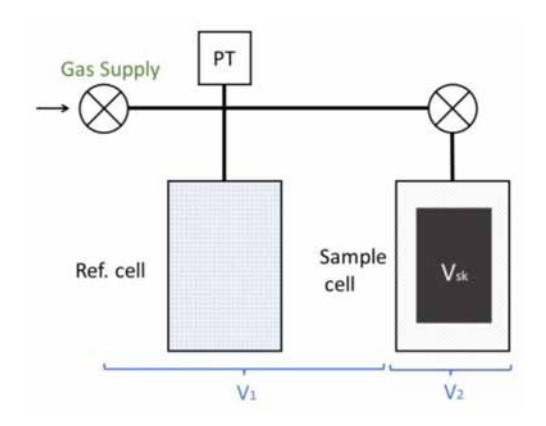


Figure 2—Manometric adsorption setup

For a single gas, the initial number of moles is (subscript "i")

$$n_i^T = \frac{P_i V_1}{z_i R T_i} + \frac{P_i^s (V_2 - V_{sk})}{z_i^s R T_i} + n_i^{exc}, \tag{3}$$

where V_1 denotes the reference volume including tubing above the connection valve, V_2 is the volume of sample cell including tubing after the valve, and "s" superscript denotes the sample cell. After opening the valve, the number of moles is (subscript "f") calculated via

$$n_f^T = + \frac{P_f V_1}{z_f R T_f} + \frac{P_f (V_2 - V_{sk})}{z_f R T_f} + n_f^{exc}. \tag{4}$$

Allowing enough time for the system to reach equilibrium ($T_i = T_f$), and considering mass balance $n_i^T = n_f^T$, the total sorption amount at final conditions is given by

$$n_f^{exc} = n_i^{exc} + \frac{1}{RT} \left[\left(\frac{P_i}{z_i} - \frac{P_f}{z_f} \right) V_1 - \left(\frac{P_f}{z_f} - \frac{P_i^s}{z_i^s} - \right) (V_2 - V_{sk}) \right]$$
 (5)

Surface area measurements. Surface area and average pore size of the activated carbon samples were measured using a surface characterization analyzer. The estimates of the activated carbon surface area and pore-size distribution are based on the BET theory developed by (Brunauer et al. 1938) that uses pure nitrogen gas to evaluate the sample surface area. Prior to performing the measurements, the samples needed to be degassed at elevated temperature of 425 K for 4 hours in order to remove moisture and any other impurities attached to the surface. The surface area measurements were conducted under 77 K by using liquid nitrogen to cool down the sample surface. This low temperature assured the strong interactions between the injected nitrogen gas and the sample surface which leads to accurate quantification of the amount of gas adsorbed onto the sample surface. The sample surface area can be finally evaluated via

$$S = \frac{X_m L_{av} A_m}{M_v},\tag{6}$$

where S is the total surface area, X_m is the monolayer capacity of the nitrogen gas adsorbed on the sample surface, L_{av} is Avogadro's number, A_m is the cross-sectional area of nitrogen gas, and M_v is the molar volume.

Molecular Dynamics Modelling

In order to build a representative molecular model for the activated carbon sample, a Crystallographic Information Framework (CIF) file has to be constructed and adjusted based on the actual properties of the actual sample. The following sections explain in detail the adopted method for building and verifying the molecular model used to simulate the adsorption isotherm of activated carbon-CO₂ system.

Construction of activated carbon molecular structures. The simulation model was built based on the physical (i.e., density, pore size, and surface area) and chemical (i.e., molecular structure and composition) properties of the tested activated carbon samples. The unit cell structure consists of linked hexagons of carbon atoms stacked in a 'ABA' sequence in which the vertical direction is perpendicular to the basal plane and the middle layer is shifted in such a way that there is a carbon atom at the center of each hexagon of the first and second layers (Trucano and Chen 1975; Serp 2013). The model consists of two parallel walls (slitpore) with three sheets of graphite forming each wall. Assuming a triclinic cell, the size of the sheets is 49.28 Å × 49.28 Å with interplanar space of 5.8 Å. The final size of the simulation cell was (a = 49.28 Å, b = 49.28 Å and c = 48.35 Å). The height of the simulation cell (i.e., parameter c) was set to 48.35 Å to account for a sample average pore size of 21.95 Å and a simulation cut-off value of 12 Å. The angles between the unit cell space vectors (α , β , and γ) are 90°, 90°, and 120°, respectively. Fig. 3 shows a schematic representation of the developed molecular model used as an input for the activated carbon simulations.

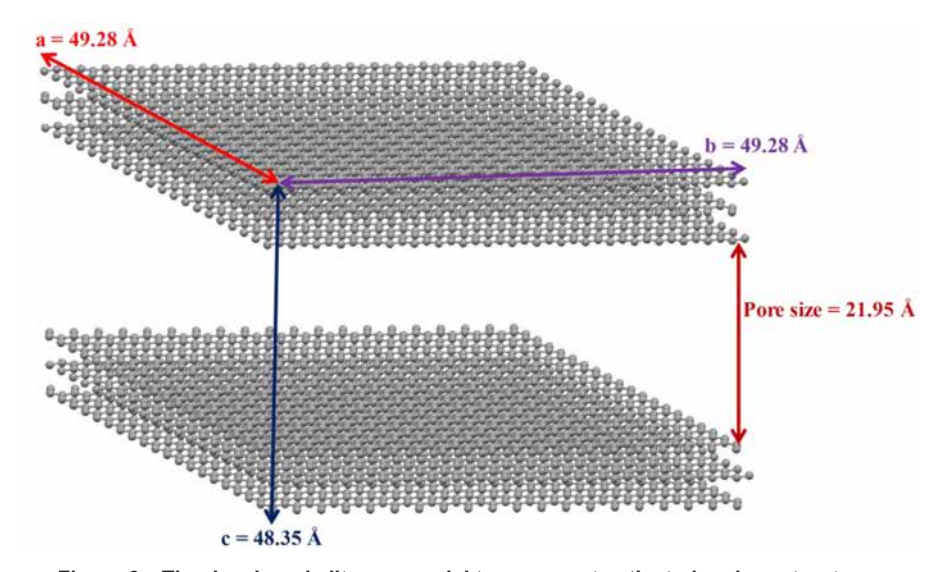


Figure 3—The developed slit-pore model to represent activated carbon structure.

Simulation environment and force fields. We used GCMC simulations for the purpose of evaluating the adsorption isotherms of CO₂ gas on the surface of the modelled activated carbon. In this paper, we used 100,000 initialization cycles by the simulation to reach the structure equilibrium conditions followed by 50,000 cycles for production. Different probabilities were assigned to Monte Carlo moves of translation (50%), reinsertion (50%) and swap (100%) trying to match the actual adsorption nature of CO₂ on the surface of activated carbon sample. A wide range of pressure values (i.e., 0.5 ? 6 MPa) was used to construct the adsorption isotherms at each specific temperature. We used RASPA software (Dubbeldam et al. 2016) to run the GCMC simulations.

Force fields were used to describe the interactions (1) among the adsorbate molecules and (2) between the adsorbate molecules and the activated carbon framework. In this paper, CO₂ molecules were represented using Transferable Potentials for Phase Equilibria (TraPPE) force filed (Potoff and Siepmann 2001), while the carbon atoms within the graphite sheets were represented by the DREIDING force field (Mayo et al. 1990). Table 1 shows the list of the force filed parameters assumed for the surface of activated carbon and

CO₂ molecules. The summation of the shifted and truncated 12-6 Lennard-Jones (LJ) and the Coulombic potentials formed the total nonbonded intermolecular potential within the system (Allen and Tildesley 1989) as

$$U = \sum_{i,j} \left[\left(\frac{\sigma_{ij}}{r_{ij}} \right)^{12} - \left(\frac{\sigma_{ij}}{r_{ij}} \right)^{6} \right] + \sum_{i,j} \frac{q_{i}q_{j}}{4\pi\varepsilon_{0}r_{ij}}, \tag{7}$$

Table 1—The assumed molecular model parameters for both activated carbon and CO2

	Atoms	σ (Å)	ε (K)	<i>q</i> (e)
Activated Carbon	С	3.34	26	0
CO ₂	C in CO ₂	2.8	27	0.7
	O in CO ₂	3.05	97	-0.35

where ε_{ij} is the depth of the potential well (dispersion energy), σ_{ij} is the collision diameter (size of the particle), and r_{ij} is the distance between atoms i and j. q_i and q_j are the atomic charges of atoms i and j, respectively, and ε_0 is the electric constant.

Lorentz-Berthelot combing rules (Maitland et al. 1983) was used to calculate the cross LJ parameters via

$$\varepsilon_{ij} = \sqrt{\varepsilon_{ii} + \varepsilon_{jj}} \tag{8}$$

and

$$\sigma_{ij} = \frac{1}{2} \left(\sigma_{ii} + \sigma_{jj} \right). \tag{9}$$

Results and Discussion

Experimental Results

Manometric setup calibration. We used five aluminum discs of known volume as blanks to carry out the calibration procedure. Fig. 4 summarizes the calibration results. From the calibration process, the reference cell volume is 18.281 cm³ and the sample cell volume is 33.719 cm³.

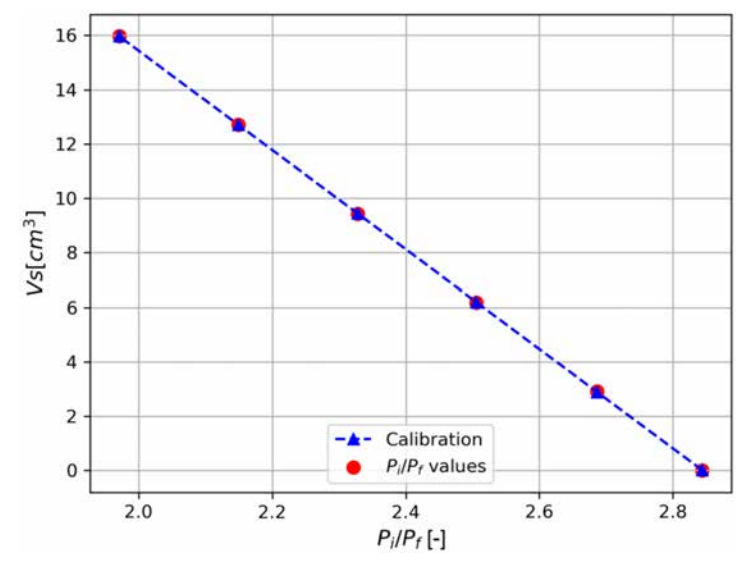


Figure 4—Manometric setup calibration results

We measured the adsorption amount of the granular activated carbon sample in the presence of CO₂. We performed the sorption experiments at a temperature of 300 K and pressures up to 6 MPa. We used two samples (S1, S2) and carried out two sorption experiments (E1, E2) per sample. Table 2 summarizes the sample properties. The sorption process started initially by pressurizing the reference cell to 2.5 MPa. After the valve was open, we allowed enough time for the system to equilibrate. The initial pressure drop corresponds to the rapid gas invasion of the macropores. The following time-dependent response correspond to the mesoporosity and microporosity.

Table 2—Activated carbon sample properties

Sample	Mass [g]	Skeletal Density [g/cm³]	Skeletal Volume [cm³]
S1	12.91	1.67	7.73
S2	13.05	1.67	7.81

Fig. 5 presents the sorption isotherms for CO_2 at 300 K on activated carbon for both samples. From this plot of excess sorption vs pressure, we observed the maximum sorption amount around 8.0 - 8.5 mmol/g occurs around a pressure of 4 MPa.

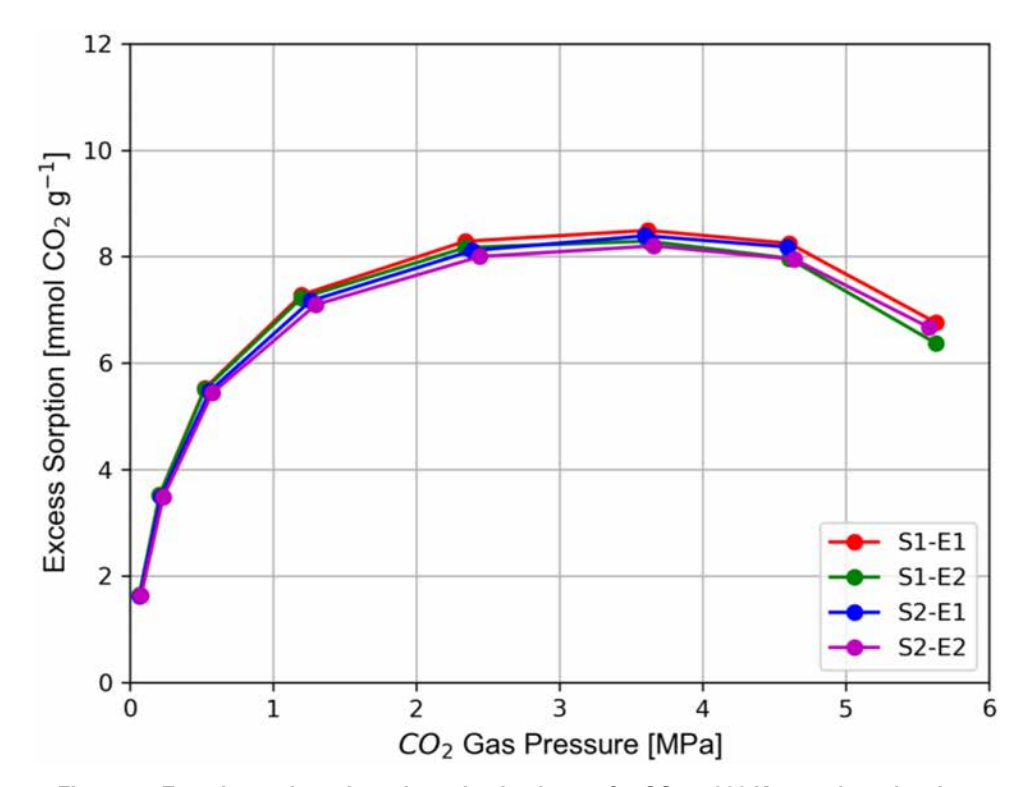


Figure 5—Experimental results: adsorption isotherms for CO₂ at 300 K on activated carbon

Our experimental results are similar to previously published CO₂ sorption isotherms for Filtrasorb F400 activated carbon at 318 K (Gensterblum et al. 2009; Pini et al. 2006; Sudibandriyo et al., 2003). These literature experiments were conducted at 318 K with CO₂ in supercritical state. These conditions resemble the conditions found in reservoirs where pressures range from 6 to 15 MPa and temperatures are in the range of 300 to 330 K (Gensterblum et al. 2009).

GCMC Simulation Results

Comparison of the experimental and molecular simulation results. The BET surface area experiments show that the tested activated carbon sample has a surface area of 1,138 m²/g with an average pore size of 21.95 Å. This reflects the wide space available for the CO₂ gas to get adsorbed to the sample surface. The average pore size of activated carbon obtained from the BET surface area experiments is in agreement with the previously documented values of the average pore size of shale-gas formations (Kuila and Prasad 2013; Zhang et al. 2016). This confirms on the validity of using activated carbon samples to study the adsorption behavior of different gases on shale formations.

Fig. 6 compares the experimental and the GCMC simulation results for the adsorption isotherm of CO₂ on the activated carbon structure at temperature of 300 K and pressure range of 0 to 5.7 MPa. The GCMC simulation results are in agreement with the adsorption experimental results given an average absolute difference of 10.6%. Both the experimental and simulation results demonstrate that the CO₂ adsorption isotherm follows the Type - I adsorption model. This observation can be explained by the nature of the pore structure of the activated carbon sample that has a wide distribution of pore sizes ranging from nano to meso scales. Fig. 7 illustrates a snapshot of the GCMC simulations of activated carbon-CO₂ system at the pressures of 0.5, 1, and 2 MPa and temperature of 300 K. It is observed that CO₂ molecules tend to adhere to the surface of the activated carbon sheets in a monolayer configuration at lower pressures. The amount of gas sorbed and stored within the pores of the activated carbon structure highly depends on the pore size of the sample. Smaller pores are completely filled with CO₂ molecules at lower pressures while more molecules accumulate in the larger pores as the pressure increases. At the pressure value of 4 MPa, the CO₂ adsorbed reaches the critical density value inside the activated carbon pores. Increasing the pressure values higher than 4 MPa leads to increase in the repulsion forces between the CO₂ molecules and hence decreases the amount of gas adsorbed on the activated carbon surface.

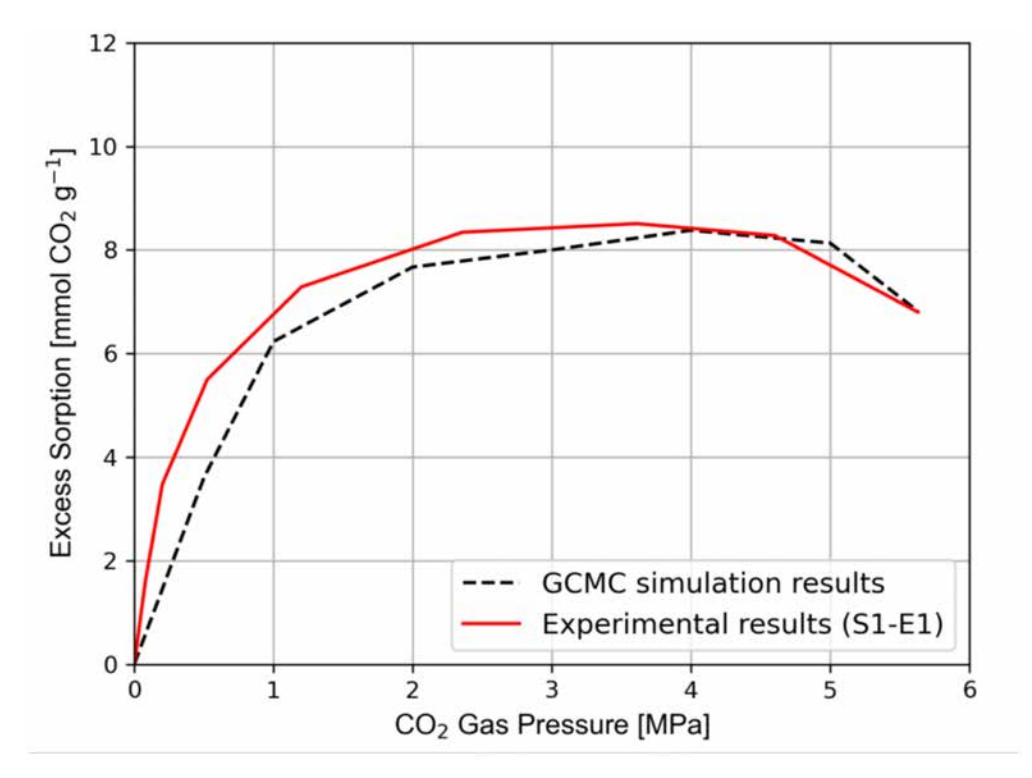


Figure 6—A comparison between the experimental and GCMC simulation of CO₂ adsorption isotherm on activated carbon surface at T = 300 K.

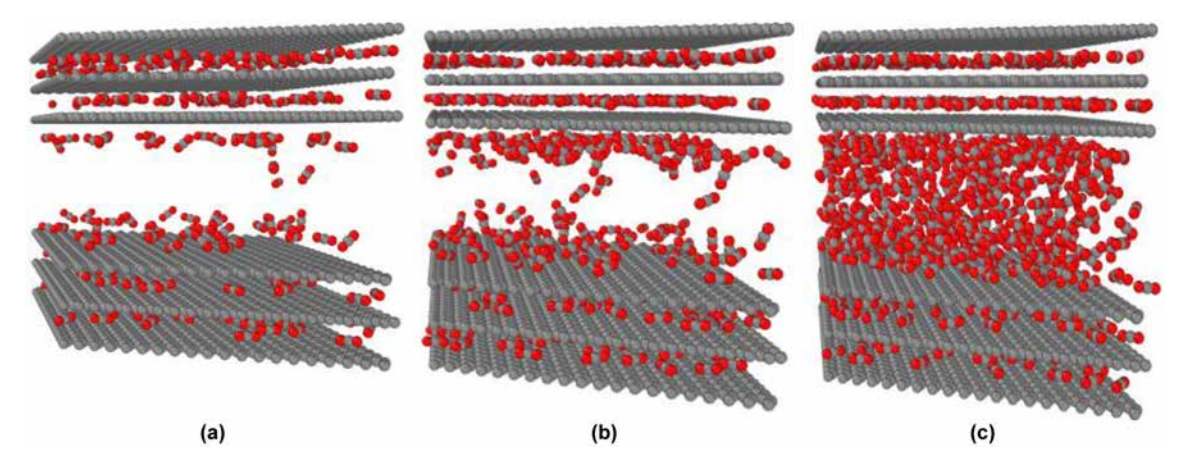


Figure 7—A snapshot of the GCMC simulation cell of CO₂ adsorption on activated carbon at T=300 K and pressure values of (a) 0.5 MPa, (b) 1 MPa, and (c) 2 MPa. The grey sheets represent the activated carbon structure (adsorbent), and the red and grey spheres represent the oxygen and carbon atoms of the CO₂ molecules, respectively.

Impact of temperature on CO₂ adsorption and storage. In order to evaluate the impact of temperature on the CO₂ adsorption on the organic matter solid interface of shale-gas reservoirs, adsorption isotherms were constructed using GCMC simulations at temperature values of 250 – 500 K and pressure values of 0.5 – 6 MPa. Fig. 8 shows the results of the excess adsorption isotherms at the indicated temperature and pressure values. Since CO₂ adsorption on the activated carbon surface is an exothermic process, CO₂ adsorption decreases as temperature increases. Therefore, for a reservoir temperature of 400 K and pressure of 2 MPa, CO₂ adsorption is expected to be 87% less than that estimated at the temperature of 300 K. This observation reflects the high dependence of CO₂ adsorption and storage in shale-gas reservoirs on the reservoir temperature. Therefore, choosing shale formations with lower temperatures and larger pore size is more viable for CO₂ sequestration projects than high-temperature reservoirs.

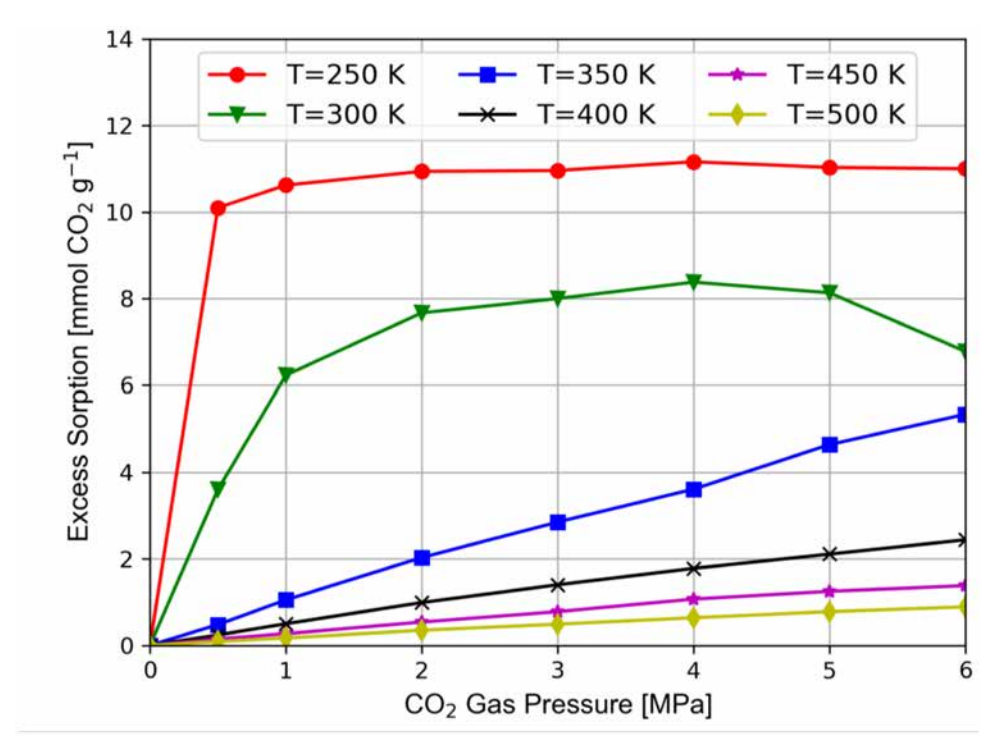


Figure 8—Activated carbon-CO₂ adsorption isotherms at temperatures of 250, 300, 350, 400, 450, and 500 K.

Effect of the presence of water vapor on CO₂ adsorption. Shale-gas reservoirs usually contain water vapor phase that affects the surface chemistry of the organic constituents of the rock. In order to represent the actual chemical composition of the organic matrix of shale-gas formations in the presence of water vapor, we implemented two different functional groups (hydroxyl – OH and carboxyl – COOH) to the surface of the activated carbon sheets. Fig. 9 compares the simulated excess CO₂ sorption isotherms in the case of pure activated carbon, activated carbon with OH functional groups, and activated carbon with COOH functional groups. It is observed that modifying the activated carbon surface with carboxyl and hydroxyl functionalities increases the CO₂ sorption capacity by 24% and 36%, respectively. This observation is attributed to the polar nature of CO₂ and the negative charges associated to these functional groups that increases the adsorption affinity of the carbon surface. Doping oxygen atoms to the surface of activated carbon makes it act as a Lewis base that can donate electrons to the acidic carbon atoms in the CO₂ molecules. This induced polarity to the activated carbon framework enhances its susceptibility to adsorb more CO₂ molecules at lower pressures through the electrostatic interactions. Moreover, the formed hydrogen bonds between the oxygen atom in CO₂ and the hydrogen atoms in the hydroxyl and carboxyl groups increases the CO₂ loading over the activated carbon surface. Therefore, the presence of water vapor on the surface of the solid rock constituents in shale-gas reservoirs positively affects the CO₂ adsorption and storage capacity.

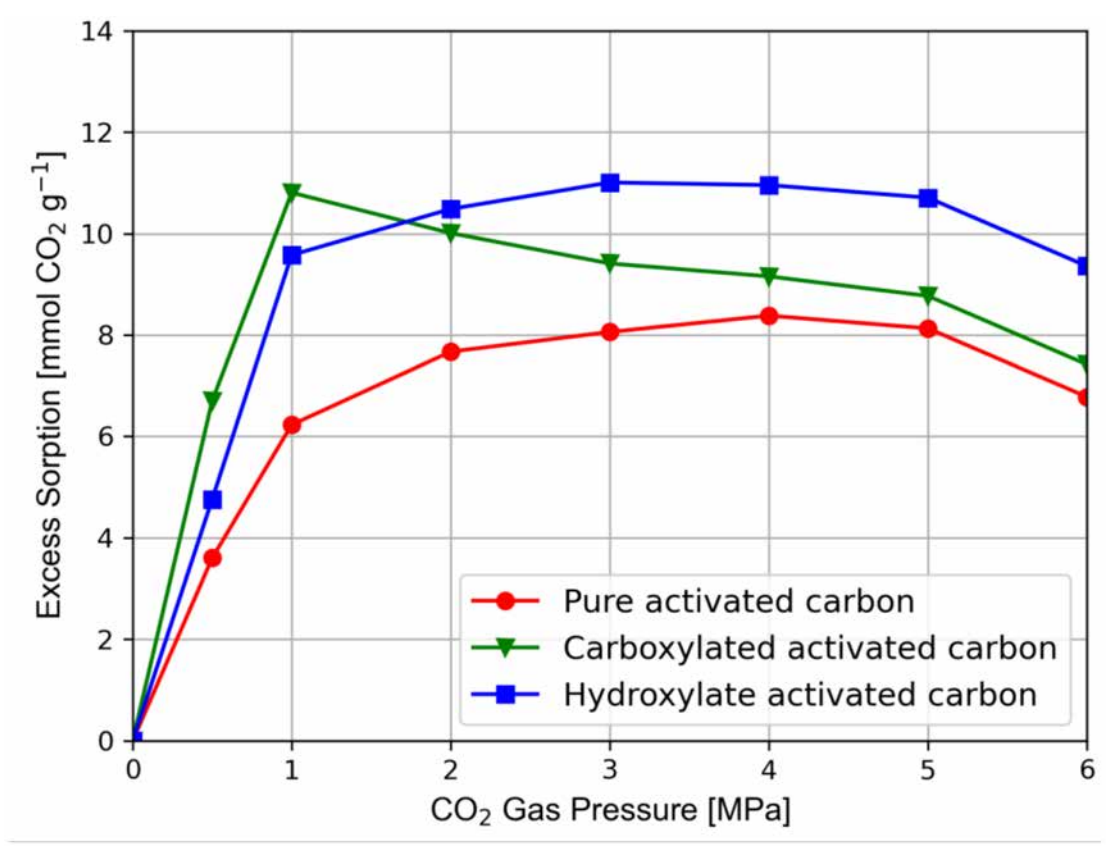


Figure 9—A comparison between the CO₂ adsorption isotherms for pure activated carbon, Carboxylated activated carbon, and Hydroxylated activated carbon at T=300 K.

Conclusions

We introduced an integrated experimental and simulation framework to quantify the impacts of major factors affecting CO_2 storage and adsorption on the surface of the organic matter present in shale-gas formations. We constructed the experimental CO_2 adsorption isotherms on activated carbon samples which had an average pore size of 21.95 Å. This pore size was shown to be analogous to the typical pore size of typical shale-gas

rocks. Then, we built a molecular-scale model to match the CO_2 adsorption isotherm on activated carbon surface using GCMC simulations. Afterwards, we used the same model to simulate the CO_2 adsorption process at different temperature values (i.e., 250-500 K). Moreover, we investigated the effect of vapor pressure on the adsorption behavior of CO_2 on activated carbon at 300 K. Finally, we addressed the impact of kerogen surface chemistry on the CO_2 adsorption and storage capacity. The main conclusions of this paper can be summarized as follows:

- Experimental estimation of high-pressure sorption amount for CO₂ has inherent challenges. Nonetheless, we were able to design a procedure that according to the present results ensures re producibility and repeatability. The agreement between the results with those in the literature validate our experimental procedure.
- Activated carbon models can reliably represent the pore structure of the organic matter content of shale-gas reservoirs. Both experimental and simulation results of CO₂ adsorption on activated carbon surface followed Type I adsorption isotherm. This observation shows how the pore structure of shale-gas formations and activated carbon have a similar pore size range with nano mesopores scale pores.
- GCMC simulations can effectively model the CO₂ adsorption process on activated carbon surface using the proper force fields. This enables running adsorption cases at extreme temperature conditions that cannot be done under conventional laboratory conditions. Moreover, GCMC simulations allowed us to carry out sensitivity analysis to quantify the effects of shale-gas surface chemistry on the CO₂ adsorption process, which was challenging to perform experimentally.
- Reservoir temperature has an inverse effect on the CO₂ adsorption on the surface of carbon sheets. Hence, an increase in temperature reduces the shale-gas capacity to store gas within its pores.
- The presence of water vapor enhances the CO₂ adsorption loading of the shale-gas reservoirs. The presence of the polar compounds (e.g., water) on the solid-fluid interface of shale-gas reservoirs makes the CO₂ molecules attached more tightly to the adsorbent surface.
- Simple activated carbon models can be used to represent the contribution of the single components (e.g., carbon) of shale-gas formations towards the CO₂ adsorption and storage process. This enables a deep understanding of the adsorption process on the molecular-scale level. However, the contribution of other structural elements should not be overlooked when evaluating the overall adsorption capacity of such complex structures.

Acknowledgements

Research reported in this paper was funded by the Joint Industry Research Program on "Multi-Scale Rock Physics" sponsored by Baker Hughes, BHP, BP, Core Laboratories, Equinor, ExxonMobil, Occidental Petroleum, Pan American Energy, and Petrobras, as well as NSF award 1834345. The authors acknowledge the Texas Advanced Computing Center (TACC) at The University of Texas at Austin for providing high performance computing resources that have contributed to the research results reported within this paper.

Acronyms

CCS = Carbon capture and sequestration

CIF = Crystallographic Information Framework

 CO_2 = Carbon dioxide

E1 = Experiment 1

E2 = Experiment 2

GCMC = Grand Canonical Monte Carlo

He = Helium

LJ = Lennard-Jones

NOAA = National Oceanic and Atmospheric Administration

PG = Pressure Gauge

PT = Pressure Transducer

RC = Reference Cell

S1 = Sample 1

S1 = Sample 2

S1-E1 = Sample 1 - Experiment 1

S1-E2 = Sample 1 - Experiment 2

SC = Sample Cell

TraPPE = Transferable Potentials for Phase Equilibria

Nomenclature

 A_m = Cross-sectional area of nitrogen gas

 L_{av} = Avogadro's number

 M_v = Nitrogen gas molar volume

 n_i^T = Total number of moles at initial conditions

 n_i^{exc} = Number of sorbed moles of gas at initial conditions

 n_t^T = Total number of moles at final conditions

 n_f^{exc} = Number of sorbed moles of gas at final conditions

 P_i = Initial Pressure

 P_{fi} = Final Pressure

 q_i = Atomic charge of atoms i

 q_i = Atomic charge of atoms j

 r_{ii} = Distance between atoms i and j

S =Sample total surface area

 T_i = Initial Temperature

 T_f = Final Temperature

U = Total nonbonded intermolecular potential

 $V_{I} = \text{Volume 1}$

 V_2 = Volume 2

 V_{sk} = Skeletal volume

 V_{sm} = Volume of solids

 $X_m =$ Monolayer capacity of the nitrogen gas adsorbed on the sample surface

 ε_0 = Electric constant

 ε_{ii} = Depth of the potential well (dispersion energy)

 σ_{ii} = Collision diameter (size of the particle)

References

Aljamaan, H., Al Ismail, M. and Kovscek, A.R. 2017. Experimental Investigation and Grand Canonical Monte Carlo Simulation of Gas Shale Adsorption from the Macro to the Nano Scale. *Journal of Natural Gas Science and Engineering*, **48**: 119–137 https://doi.org/10.1016/j.jngse.2016.12.024.

Allen, M.P. and Tildesley, D.J. 1989. Computer Simulation of Liquids, second edition, Oxford: Oxford University Press.
Bhui, U.K.2021. Hydrocarbon Cycle for Sustainable Future: Clean Energy and Green Environment of the Earth. In Macromolecular Characterization of Hydrocarbons for Sustainable Future: Ap-plications to Hydrocarbon Value Chain, ed. Bhui, U. K., 3–18. Singapore: Springer. https://doi.org/10.1007/978-981-33-6133-1_1.

Boosari, S.S.H., Aybar, U. and Eshkalak, M.O.2015. Carbon Dioxide Storage and Sequestration in Un-conventional Shale Reservoirs. *Journal of Geoscience and Environment Protection*, **3**: 7–15. https://doi.org/10.4236/gep.2015.31002.

Brunauer, S., Emmett, P.H. and Teller, E. 1938. Adsorption of Gases in Multimolecular Layers. *Journal of the American Chemical Society*, **60**: 309–319 https://doi.org/10.1021/ja01269a023.

- Chalmers, G.R.L. and Bustin, R.M.2008. Lower Cretaceous Gas Shales in Northeastern British Columbia, Part I: geological controls on methane sorption capacity. *Bulletin of Canadian Petroleum Geology*, **56** (1): 1–21. https://doi.org/10.2113/gscpgbull.56.1.1.
- Cristancho-Albarracin, D., Akkutlu, I.Y., Criscenti, L.J. and Wang, Y.2017. Shale Gas Storage in Kerogen Nanopores with Surface Heterogeneities. *Applied Geochemistry*, **84**: 1–10. https://doi.org/10.1016/j.apgeochem.2017.04.012.
- Dubbeldam, D., Calero, S., Ellis, D.E. and Snurr, R.Q.2016. RASPA: Molecular Simulation Software for Adsorption and Diffusion In Flexible Nanoporous Materials. *Molecular Simulation*, **42**: 81–101 https://doi.org/10.1080/08927022.2015.1010082.
- Edmonds, J.A., Freund, P.F. and Dooley, J.J.2002. The Role of Carbon Management Technologies in Addressing Atmospheric Stabilization of Greenhouse Gases. Report, Pacific Northwest National Lab., Richland, Washington.
- Gensterblum, Y., Van Hemert, P., Billemont, P., Busch, A., Charriére, D., Li, D., Krooss, B., De Weireld, G., Prinz, D., Wolf, K.-H. 2009. European Inter-Laboratory Comparison of High Pressure CO₂ Sorption Isotherms. I: Activated Carbon. *Carbon* 47: 2958–2969.
- He, Y., Manful, D. et al 2022. Quantification of Impacts Between 1.5 and 4 °C of Global Warming on Flooding Risks in Six Countries. *Climatic Change*, **170** (15). https://doi.org/10.1007/s10584-021-03289-5.
- Heller, R. and Zoback, M.2014. Adsorption of methane and carbon dioxide on gas shale and pure mineral samples. *Journal of Unconventional Oil and Gas Resources*, **8**: 14–24. https://doi.org/10.1016/j.juogr.2014.06.001.
- Hemert, P., Bruining, H., Rudolph, E.S.J., Wolf, K.A.A., and Mass, J.G. 2009. Improved Manometric Setup for the Accurate Determination of Supercritical Carbon Dioxide Sorption, *Review of Scientific Instruments*, **80** (3): 035103.
- Jagadisan, A., de Araujo, I.S. and Heidari, Z. 2021. Impact of Kerogen Geochemistry on Methane and Water Adsorption Using Molecular Simulations. Paper presented at the SPE/AAPG/SEG the 9th Unconventional Resources Technology Conference, Houston, Texas, USA, 26–28 July. UR-TEC-2021-5350-MS. https://doi.org/10.15530/urtec-2021-5350.
- Johansson, T., Williams, R., Ishitani, H. and Edmonds, J.A. 1996. Options for Reducing CO₂ Emissions from the Energy Supply Sector. *Energy Policy*, **24**: 985–1003 https://doi.org/10.1016/S0301-4215(96)80362-4.
- Khosrokhavar, R., Griffiths, S. and Wolf, K.-H. 2014. Shale Gas Formations and Their Potential for Carbon Storage: Opportunities and Outlook. *Environmental Processes*, 1: 595–611. https://doi.org/10.1007/s40710-014-0036-4.
- Kuila, U. and Prasad, M.2013. Specific Surface Area and Pore-Size Distribution in Clays and Shales. *Geophysical Prospecting*, **61**: 341–362 https://doi.org/10.1111/1365-2478.12028.
- Kumar, A., Ozah, R., Noh, M., Pope, G.A., Bryant, S., Sepehrnoori, K. and Lake, L.W. 2005. Reservoir Simulation of CO₂ Storage in Deep Saline Aquifers. *SPE Journal*, **10**: 336–348 SPE-89343-PA. https://doi.org/10.2118/89343-PA.
- Lau, H.C., Ramakrishna, S., Zhang, K. and Radhamani, A.V.2021. The Role of Carbon Capture and Storage in the Energy Transition. *Energy & Fuels*, **35**: 7364–7386 https://doi.org/10.1021/acs.energyfuels.1c00032.
- Li, Z., Dong, M., Li, S. and Huang, S. 2006. CO₂ Sequestration in Depleted Oil and Gas Reservoirs—Caprock Characterization and Storage Capacity. *Energy Conversion and Management*, **47**: 1372–1382 https://doi.org/10.1016/j.enconman.2005.08.023.
- Liu, H., Rao, X. and Xiong, H. 2020. Evaluation of CO₂ Sequestration Capacity In Complex-Boundary-Shape Shale Gas Reservoirs Using Projection-Based Embedded Discrete Fracture Model (pEDFM). *Fuel*, **277**: 118201. https://doi.org/10.1016/j.fuel.2020.118201.
- Liu, Y. and Wilcox, J. 2012. Effects of Surface Heterogeneity on the Adsorption of CO₂ in Microporous Carbons. *Environmental Science & Technology*, **46**: 1940–1947 https://doi.org/10.1021/es204071g.
- Maitland, G., Rigby, M., Smith, E., Wakeham, W. and Henderson, D.1983. Intermolecular Forces: Their Origin and Determination. *Physics Today*, **36**: 57–58 https://doi.org/10.1063/1.2915587.
- Mayo, S.L., Olafson, B.D. and Goddard, W.A. 1990. DREIDING: A Generic Force Field for Molecular Simulations. *The Journal of Physical Chemistry*, **94**: 8897–8909 https://doi.org/10.1021/j100389a010.
- Merey, S. and Sinayuc, C.2016. Analysis of Carbon Dioxide Sequestration in Shale Gas Reservoirs by Using Experimental Adsorption Data and Adsorption Models. *Journal of Natural Gas Science and Engineering*, **36**: 1087–1105 https://doi.org/10.1016/j.jngse.2016.02.052.
- Mosher, K., He, J., Liu, Y., Rupp, E. and Wilcox, J.2013. Molecular Simulation of Methane Adsorption in Micro and Mesoporous Carbons with Applications to Coal and Gas Shale Systems. *International Journal of Coal Geology*, 109–110: 36–44. https://doi.org/10.1016/j.coal.2013.01.001.
- Pini, R., Ottiger, S., Rajendran, A., Storti, G., Mazzotti, M.2006. Reliable measurement of near-critical adsorption by gravimetric method. *Adsorption: Journal of the International Adsorption Society*, **12**:393–403.
- Potoff, J.J. and Siepmann, J.I.2001. Vapor–Liquid Equilibria of Mixtures Containing Alkanes, Carbon Dioxide, and Nitrogen. *AIChE Journal*, 47: 1676–1682 https://doi.org/10.1002/aic.690470719.

Sandoval, D.R., Yan, W., Michelsen, M.L. and Stenby, E.H.2018. Modeling of Shale Gas Adsorption and Its Influence on Phase Equilibrium. *Industrial & Engineering Chemistry Research*, **57**: 5736–5747 https://doi.org/10.1021/acs.iecr.7b04144.

- Serp, P. 2013. Carbon. In *Comprehensive Inorganic Chemistry II* (Second Edition), ed. Reedijk, J. and Poeppelmeier, K. 323–369. Amsterdam: Elsevier. https://doi.org/10.1016/B978-0-08-097774-4.00731-2.
- Shi, J.Q. and Durucan, S. 2005. CO₂ Storage in Deep Unminable Coal Seams. *Oil & Gas Science and Technology*, **60**: 547–558 https://doi.org/10.2516/ogst:2005037.
- Shirbazo, A., Taghavinejad, A. and Bagheri, S. 2021. CO₂ Capture and Storage Performance Simulation in Depleted Shale Gas Reservoirs as Sustainable Carbon Resources. *Journal of Construction Materials*. https://doi.org/10.36756/JCM.si1.3.
- Steffen, W., Rockström, J.et al 2018. Trajectories of the Earth System in the Anthropocene. *Proceedings of the National Academy of Sciences*, **115**: 8252–8259. https://doi.org/10.1073/pnas.1810141115.
- Sudibandriyo, M., Pan, Z., Fitzgerald, J.E., Robinson R.L., Jr, Gasem, KAM. 2003. Adsorption of methane, nitrogen, carbon dioxide, and their binary mixtures on dry activated carbon at 318.2 K and pressures up to 13.6 MPa. *Langmuir*, 19:5323–31.
- Sui, H. and Yao, J. 2016. Effect of Surface Chemistry for CH₄/CO₂ Adsorption in Kerogen: A Molecular Simulation Study. *Journal of Natural Gas Science and Engineering*, **31**: 738–746 https://doi.org/10.1016/j.jngse.2016.03.097.
- Tayari, F., Blumsack, S., Dilmore, R. and Mohaghegh, S.D. 2015. Techno-economic Assessment of Industrial CO₂Storage in Depleted Shale Gas Reservoirs. *Journal of Unconventional Oil and Gas Resources*, **11**: 82–94 https://doi.org/10.1016/j.juogr.2015.05.001.
- Trucano, P. and Chen, R.1975. Structure of Graphite by Neutron Diffraction. *Nature*, **258**: 136–137. https://doi.org/10.1038/258136a0.
- Vilarrasa, V., Bolster, D., Olivella, S. and Carrera, J. 2010. Coupled Hydromechanical Modeling of CO₂Sequestration in Deep Saline Aquifers. *International Journal of Greenhouse Gas Control*, **4**: 910–919. https://doi.org/10.1016/j.ijggc.2010.06.006.
- Wang, T., Tian, S., Li, G., Zhang, L., Sheng, M. and Ren, W.2021. Molecular Simulation of Gas Adsorption in Shale Nanopores: A Critical Review. *Renewable and Sustainable Energy Reviews*, **149**: 111391. https://doi.org/10.1016/j.rser.2021.111391.
- White, C.M., Strazisar, B.R., Granite, E.J., Hoffman, J.S. and Pennline, H.W. 2003. Separation and Capture of CO₂ from Large Stationary Sources and Sequestration in Geological Formations—Coalbeds and Deep Saline Aquifers. *Journal of the Air & Waste Management Association*, **53**: 645–715 https://doi.org/10.1080/10473289.2003.10466206.
- Yao, J., Sun, H., Fan, D., Wang, C. and Sun, Z.2013. Numerical Simulation of Gas Transport Mechanisms in Tight Shale Gas Reservoirs. *Petroleum Science*, **10**: 528–537 https://doi.org/10.1007/s12182-013-0304-3.
- Yun, J.-H., He, Y., Otero, M., Düren, T. and Seaton, N.A. 2002. Adsorption Equilibrium of Polar/Non-Polar Mixtures on MCM-41: Experiments and Monte Carlo Simulation. In *Studies in Surface Science and Catalysis, Characterization* of Porous Solids VI, 685–692, ed. Rodriguez-Reinoso, F., McEnaney, B., Rouquerol, J. and Unger, K. https://doi.org/10.1016/S0167-2991(02)80197-5.
- Zhan, H., Wu, S., Bao, R., Zhao, K., Xiao, L., Ge, L. and Shi, H.2015. Water Adsorption Dynamics in Active Carbon Probed by Terahertz Spectroscopy. *RSC Advances*, **5**: 14389–14392. https://doi.org/10.1039/C4RA14730H.
- Zhang, H., Bucior, B.J. and Snurr, R.Q. 2018. Molecular Modeling of Carbon Dioxide Adsorption in Metal-Organic Frameworks. In *Modelling and Simulation in the Science of Micro- and Meso-Porous Materials*, ed. Catlow, C. R. A., Van Speybroeck, V. and van Santen, R. A., Chap. 4, 99–149. Elsevier. https://doi.org/10.1016/B978-0-12-805057-6.00004-1.
- Zhang, H., Zeng, X., Zhao, Z., Zhai, Z. and Cao, D. 2017a. Adsorption and Selectivity of CH₄/CO₂ in Functional Group Rich Organic Shales. *Journal of Natural Gas Science and Engineering*, **39**: 82–89 https://doi.org/10.1016/j.jngse.2017.01.024.
- Zhang, T., He, Y., Yang, Y. and Wu, K. 2017b. Molecular Simulation of Shale Gas Adsorption in Organic Matter Nanopore. *Journal of Natural Gas Geoscience*, **2**: 323–332. https://doi.org/10.1016/j.jnggs.2018.01.001.
- Zhang, Y., Shao, D., Yan, J., Jia, X., Li, Y., Yu, P. and Zhang, T.2016. The Pore Size Distribution and Its Relationship with Shale Gas Capacity in Organic-Rich Mudstone of Wufeng-Longmaxi Formations, Sichuan Basin, China. *Journal of Natural Gas Geoscience*, 1: 213–220. https://doi.org/10.1016/j.jnggs.2016.08.002.
- Zhou, J., Liu, M., Xian, X., Jiang, Y., Liu, Q. and Wang, X. 2019. Measurements and Modelling of CH₄ and CO₂ Adsorption Behaviors on Shales: Implication for CO₂ Enhanced Shale Gas Recovery. *Fuel*, **251**: 293–306 https://doi.org/10.1016/j.fuel.2019.04.041.